Cellular Physiology and Biochemistry

Cell Physiol Biochem 2017;43:1288-1300
DOI: 10.1159/000481841
Published online: October 09, 2017
Accepted: July 25, 2017

Original Paper

Ultrastructural, Confocal and Viscoelastic Characteristics of Whole Blood and Plasma After Exposure to Cadmium and Chromium Alone and in Combination: An *Ex Vivo* Study

Chantelle Venter[a] Hester Magdalena Oberholzer[a] Janette Bester[b]
Mia-Jeanne van Rooy[b] Megan Jean Bester[a]

[a]Department of Anatomy, Faculty of Health Sciences, University of Pretoria, Pretoria [b]Department of Physiology, Faculty of Health Sciences, University of Pretoria, Pretoria, South Africa

Key Words
Heavy metals • Cadmium • Chromium • Erythrocytes • Fibrin fibres • Platelets • Thromboelastography • Scanning electron microscopy • Confocal microscopy

Abstract
Background/Aims: Heavy metal pollution is increasing in the environment, contaminating water, food and air supplies. This can be linked to many anthropogenic activities. Heavy metals are absorbed through the skin, inhalation and/or orally. Irrespective of the manner of heavy metal entry in the body, the blood circulatory system is potentially the first to be affected following exposure and adverse effects on blood coagulation can lead to associated thrombotic disease. Although the plasma levels and the effects of cadmium (Cd) and chromium (Cr) on erythrocytes and lymphocytes have been described, the environmental exposure to heavy metals are not limited to a single metal and often involves metal mixtures, with each metal having different rates of absorption, different cellular, tissue, and organ targets. Therefore the aim of this study is to investigate the effects of the heavy metals Cd and Cr alone and whether Cr synergistically increases the effect of Cd on physiological important processes such as blood coagulation. ***Methods:*** Human blood was exposed to the heavy metals *ex vivo*, and thereafter morphological analysis was performed with scanning electron- and confocal laser scanning microscopy (CLSM) in conjunction with thromboelastography®. ***Results:*** The erythrocytes, platelets and fibrin networks presented with ultrastructural changes, including varied erythrocytes morphologies, activated platelets and significantly thicker fibrin fibres in the metal-exposed groups. CLSM analysis revealed the presence of phosphatidylserine on the outer surface of the membranes of the spherocytic erythrocytes exposed to Cd and Cr alone and in combination. The viscoelastic analysis revealed only a trend that indicates that clots that will form after heavy metal exposure, will likely be fragile and unstable especially for Cd and Cr in combination. ***Conclusion:*** This study identified the blood as an important target system of Cd and Cr toxicity.

H.M. Oberholzer

Department of Anatomy, Faculty of Health Sciences, University of Pretoria
Private Bag x323, Arcadia 0007, (South Africa)
E-Mail nanette.oberholzer@up.ac.za

KARGER

Introduction

Haemostasis is important to ensure the recovery of injured blood vessels and to prevent excessive blood loss and this process is tightly regulated to prevent the formation of occlusive thrombi in blood vessels [1], that may lead to for example stroke [2]. The classic coagulation pathway introduced in 1964 focused on the role of the coagulation factors in thrombus formation, and ignored the role of cellular elements in the activation of the coagulation system and for this reason a new model that includes platelets and tissue factor expressing cells known as the cell-based model of coagulation was introduced. The phases of the cell-based coagulation pathway include initiation, amplification and propagation, which contribute to the formation of the clot, with platelets playing a crucial role in this process [1, 3, 4]. Platelets are involved in the release of certain factors and enzymes that contribute to clot formation and the tautness of the fibrin fibres [3, 4]. The formed thrombus consists of platelets, fibrin fibres and erythrocytes that determine the structure and integrity of the clot.

Apoptosis is well described for nucleated cells, but recently this process of programmed cell death has also been described for enucleate cells such as erythrocytes and platelets. In erythrocytes this process is known as eryptosis [5-11]. Characteristic features of this process are cell membrane shrinkage as well as blebbing and membrane scrambling [11]. During clot formation erythrocytes assist in bringing platelets to the surface of an injured vessel wall and binding inflammatory mediators to surface receptors [12]. Other cells that are involved in clot formation are the leukocytes that comprise of neutrophils, monocytes, lymphocytes, basophils and eosinophils [13], of which only the neutrophils and monocytes play a major role in the inflammatory response of the body. Leukocytes functions during coagulation include: changes in the expression of membrane receptors, release inflammatory mediators, releases oxidants like hydrogen peroxide (H_2O_2) and superoxide anion ($O_2\bullet$) and when leucocytes associate with platelets it may lead to mutual activation and protection form inhibitors [13].

Platelets and the fibrin network play an important role in the formation and stability of haemostasis. Platelet activation induces shape changes and aggregation that also leads to fibrin formation. Fibrin formation is the final step in blood coagulation and is necessary for clot stability. Fibrin formation is catalysed by thrombin, as it converts fibrinogen to fibrin [14, 15]. Changes to the morphology of erythrocytes, platelet activation and fibrin fibre thickness, caused by exposure to various substances, like smoking, heavy metals, carbon monoxide, sulfur dioxide and the presence of certain disease conditions, may alter the haemostatic process leading to the formation of pathological thrombi [11, 14, 16-20].

Environmental exposure to heavy metals via water, food and air pollution due to agriculture, mining, transport and related operations as well as cigarette smoking, a major non-occupational source of metals such as cadmium (Cd) and chromium, (Cr), are increasing [21-23]. These heavy metals have the potential to adversely affect blood homeostasis especially of those living close to high-risk areas [24]. Exposure is usually not to a single metal but as a mixture of metals [24]. Therefore the aim of this study was to determine, using and *ex vivo* blood model, the effects of Cd and Cr alone and in combination on the morphology of erythrocytes, platelet activation and fibrin fibre thickness, by using scanning electron microscopy (SEM), confocal laser scanning microscopy (CLSM) and thromboelastography® (TEG®).

Materials and Methods

Ex vivo model

Human blood was collected from six healthy consenting donors by a trained phlebotomist (Health Sciences Research Ethics Committee number: 111/2016). The inclusion criteria were: Healthy male individuals over the age of 18 years, non-smokers, that are not taking chronic medication and do not have inflammatory conditions.

Scanning electron microscopy

SEM was used to study the erythrocyte, platelet and fibrin fibre morphology. The micrographs of fibrin networks were used to analyse fibrin fibre thickness. For morphological analysis whole blood (WB) and platelet-rich plasma (PRP) was used [25]. Human blood was collected in citrate tubes and 900µℓ of WB was placed in an Eppendorf tube and exposed to 100µℓ of 48mg/ℓ cadmium chloride ($CdCl_2$) [Merck (Pty) Ltd, South Africa] and/or 1450mg/ℓ potassium dichromate ($K_2Cr_2O_7$) [Merck (Pty) Ltd, South Africa]. The metal concentrations were made up in isotonic phosphate buffered saline (pH=7.4) (*iso*PBS). The final osmolality of all solutions were less than 300mOsm to ensure any observed effects were directly due to metal toxicity. The final exposure concentrations were 4.8mg/ℓ for Cd (26µM) and 145mg/ℓ for (985µM) for Cr(VI) [26]. These concentrations where chosen based on the World Health Organization (WHO) acceptable water limits (mg/ℓ) for Cd and Cr times 1000 [26]. Both Cd and Cr are at ratios that are representative of these established limits. By using a 1000x higher concentration and short exposure times, specific cellular targets can be identified which later can be evaluated in models of chronic exposure. The control blood was exposed to *iso*PBS.

The WB was exposed for 10 minutes, before 10µℓ of WB was placed on a 10mm coverslip (LeicaSA), with and without the addition of 5µℓ of human thrombin (20U/mℓ; South African National Blood Service). The WB was then centrifuged at 227xg for 10 minutes to obtain PRP; where after 10µℓ of the PRP was placed on coverslips, with and without 5µℓ of thrombin. The cover slips were placed in 24-well plates that contained 0.075M sodium potassium phosphate buffer solution (PBS) (pH=7.4). The samples were washed for 20 minutes on a shaker to remove any blood proteins that might be trapped within the blood clots [25]. The washed samples were fixed in 2.5% glutaraldehyde and formaldehyde for 30 minutes. This was followed by rinsing of the samples, three times in PBS for 3 minutes, before secondary fixation in 1% osmium tetroxide (OsO_4) for 15 minutes. The samples were washed again as described above, where after it was serially dehydrated in 30%, 50%, 70%, 90% and 3 times in 100% ethanol. The SEM sample preparation was completed by drying the samples in hexamethyldisilazane (HMDS), followed by mounting and coating with carbon, and examining using the Zeiss Crossbeam 540 FEG-SEM and Zeiss Ultra Plus FEG-SEM (Carl Zeiss Microscopy, Munich, Germany). The thickness of the fibrin fibres was measured on the micrographs using ImageJ (Version 1.49, Java) [25]. Fifty random fibres were measured per volunteer in the control- and metal exposed groups.

Confocal laser scanning microscopy

The CLSM was used to detect phosphatidylserine (PS) on the erythrocyte membrane indicating that eryptosis is taking place. Annexin V was used to mark PS on the surface of the membrane. The blood was collected in citrate tubes and the control were ones again only exposed to *iso*PBS and for the metal groups were exposed to the metals dissolved in *iso*PBS, as described above. The positive control was Melittin (GenScript, New Jersey, USA), an apoptosis inducing peptide [27-29], to which the blood was exposed for four hours. The blood was then centrifuged at 145xg`s for ten minutes at room temperature to collect the erythrocytes. The supernatant was removed and the remaining erythrocyte pellet was washed twice with PBS for 3 minutes. The blood was then washed with the Annexin V binding buffer (BioLegend, 422201) also for 3 minutes. 5µℓ of the Annexin V probe (BioLegend, 640906) was added to the binding buffer and incubated at room temperature, protected from light, for 90 minutes. After incubation the samples were washed again as described with the phosphate- and binding buffers, to remove any unbound antibodies. 10µℓ of the prepared sample was mounted on a glass slide and covered with a coverslip (LeicaSA). The sample was viewed with the Zeiss LSM 880 confocal laser scanning microscope in Airyscan mode (Carl Zeiss Microscopy, Munich, Germany).

To visualize the erythrocytes, two different lasers were used with different filters and beam splitters, to allow the overlaying of the respective images to show which erythrocytes have a PS flip present on the membrane. For the auto-fluorescence of all the cells present on the slide, the 405nm laser was used to excite naturally occurring fluorescence found in erythrocytes and a red colour was assigned to this fluorescent signal. In an unstained sample, the 405nm laser was used together with the 465nm-505nm band pass (BP) and 525nm long pass (LP) filters and the 488nm/405nm beam splitters. These settings showed that all the erythrocytes present on the slide has auto-fluorescence, and this auto-fluorescence could therefore be used as a contrasting method against the Annexin-V binding, in the case where PS flip is present. To visualize Annexin-V binding (excitation wavelength: 494nm and emission wavelength: 518nm), the 488nm laser was

used with the 420nm-480nm/495nm-550nm BP filters and the 488nm/405nm beam splitters, and showed a green fluorescence, indicating the presence of a PS flip on the erythrocyte membranes.

Viscoelastic analysis

TEG® is an analytic method by which the viscoelastic changes that occur during coagulation and fibrinolysis are measured. The results from the blood samples are generated by the TEG® through a rotating pin, which constantly measures the resistance of the forming clot on the pin, that indicates a number of characteristics of the coagulation system such as the speed and strength of clot formation [30-32]. The results are displayed as a graph that gives various measurements of the parameters that are listed in Table 1. For this study, blood was collected in citrate tubes and exposed, as described above, where after 340µℓ of the WB was placed in a cup of the TEG® (TEG® 5000 computer-controlled device, Haemoscope Crop., Niles, IL, USA), together with 20µℓ of 0.2M calcium chloride ($CaCl_2$) to activate the coagulation process [25]. The process was allowed to run until MA was reached, since only the rate and strength of clot formation was relevant to this study.

Table 1. TEG parameters typically generated for whole blood (modified from: [33])

Thromboplastic parameters	Description
R: Reaction time	Time of latency from start of test to initial fibrin formation (amplitude of 2 mm); i.e. initiation time
K: Kinetics	Time taken to achieve a certain level of clot strength (amplitude of 20 mm); i.e. amplification
α angle: Alpha angle (slope between the traces represented by R and K)	The angle measures the speed at which fibrin build up and cross linking takes place, hence assesses the rate of clot formation; i.e. thrombin burst
MA: Maximal amplitude	Maximum strength/stiffness of clot. Reflects the ultimate strength of the fibrin clot, i.e. overall stability of the clot
MRTG: Maximum rate of thrombus generation	The maximum velocity of clot growth observed or maximum rate of thrombus generation using G, where G is the elastic modulus strength of the thrombus in dynes per cm^{-2}
TMRTG: Time to maximum rate of thrombus generation	The time interval observed before the maximum speed of the clot growth
TTG: Total thrombus generation	The clot strength: the amount of total resistance (to movement of the cup and pin) generated during clot formation. This is the total area under the velocity curve during clot growth, representing the amount of clot strength generated during clot growth

Statistical analysis

Statistical analysis of the SEM fibrin fibre thickness and TEG® parameters were performed on GraphPad Prism Version 6.01 using one-way ANOVA and Tukey's multiple comparisons test, where a p-value of ≤ 0.05 was considered to be significant.

Results

Scanning electron microscopy

Fig. 1 represents the erythrocytes identified in the various groups. In Fig. 1A normal erythrocyte morphology is seen, with minimal eryptotic erythrocytes, the predominant morphology observed in the control group. A variety of erythrocyte morphologies were present in the Cd, Cr and Cd and Cr groups, including spherocytes (Fig. 1B), echinocytes and knizocytes (Fig. 1C and D respectively). Fig. 2 represents the platelets seen in the various groups included in this study. Fig. 2A shows normal platelets with minimal changes

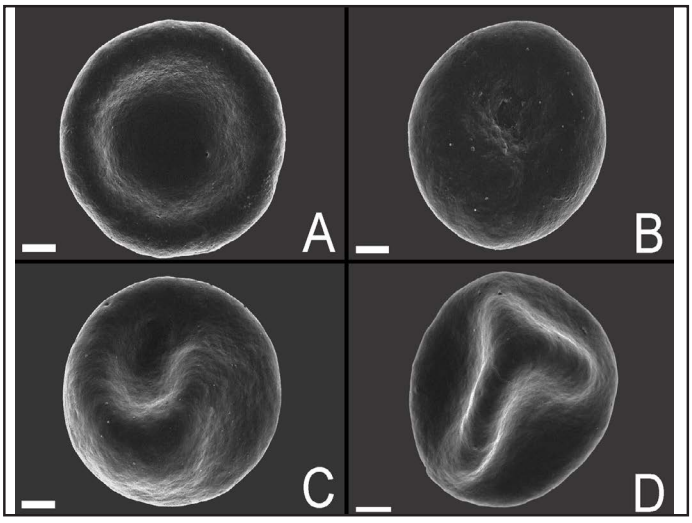

Fig. 1. Representative scanning electron micrographs of erythrocytes of the control and metal exposed groups. Fig.s A (control) shows the normal concaved morphology of an erythrocyte, with Fig.s B (Cd), C (Cr), and D (Cd and Cr) showing the changes that occurred after metal exposure (Scale bars: 1µm).

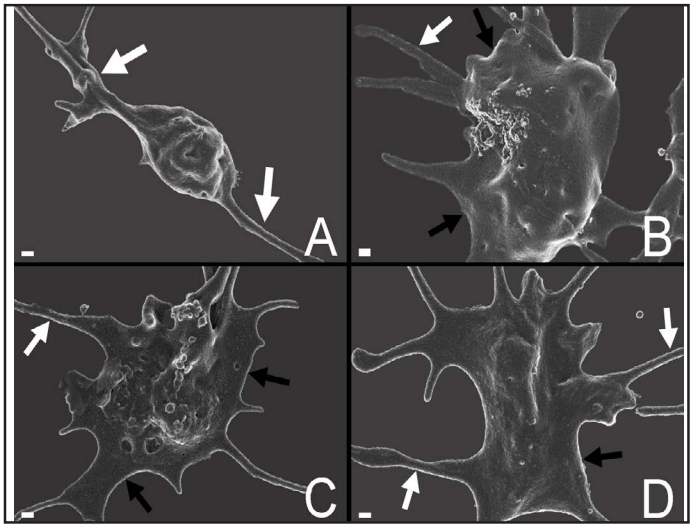

Fig. 2. Representative scanning electron micrographs of platelets from the control and metal groups. Fig. A shows a typical control platelet with pseudopodia and Fig.s B (Cd), C (Cr) and D (Cd and Cr), indicating both pseudopodia and membrane spreading. White arrows: Pseudopodia; Black arrows: Membrane spreading (Scale bars: 200nm).

to platelet shape and pseudopodia (white arrows). Minor activation is expected as contact activation will occur during sample preparation. Fig. 2B (Cd), C (Cr) and D (Cd and Cr) show activated platelets in all the metal exposed groups, with pseudopodia (white arrows) and platelet spreading (black arrows). There also appears to be an increase in the occurrence of membrane alterations, i.e. granular appearing membranes, visible in the experimental groups. Fig. 3 shows representative fibrin networks obtained in each group. In Fig. 3A a typical control fibrin network can be seen, with mostly taut, straight fibres and a combination of thin and thick fibrin fibres (red and white arrows). Figures 3B, C and D show abnormal fibrin networks that are less taut or bent fibres (blue arrows). Fig. 4 illustrates the effects of the metals on the entire coagulation system, which shows the interactions between the erythrocytes and fibrin fibres. Fig. 4A shows the normal erythrocyte morphology with minimal fibre interaction. With exposure to metals, erythrocyte morphology is altered with increased formation of spherocytes, echinocytes and knizocytes and associated interaction between the erythrocytes and fibrin fibres [Fig. 4B, C and D (blue arrows)]. Table 2 summarises the effects of the metals on the coagulation system.

Fig. 5 shows the results obtained from the measurement of the fibrin fibre thickness. The fibres in the group exposed to Cr alone and Cd and Cr in combination are statistically thicker than the Cd fibrin fibres, but are similar in thickness compared to the control group.

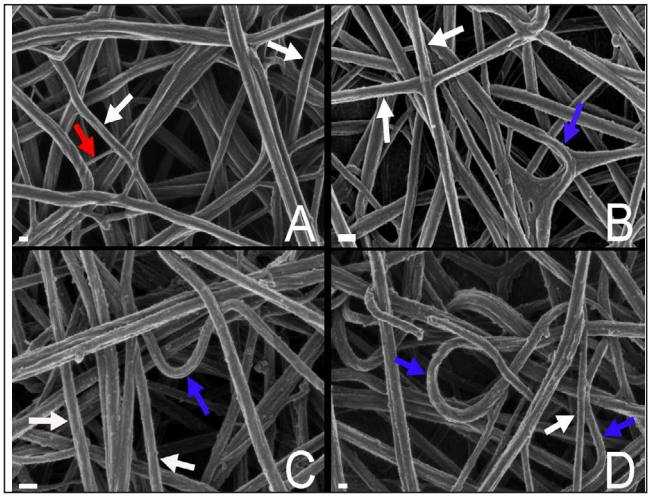

Fig. 3. Representative scanning electron micrograph of the fibrin networks of the control and metal groups. Fig. A (control) shows a combination of thick and thin fibres, with Fig.s B (Cd), C (Cr) and D (Cd and Cr) indicating the changes observed after metal exposure. White arrow: Major thick fibre; Red arrow: minor thin fibre; Blue arrow: Bend/loose fibre (Scale bars: A and D: 100nm; B and C: 200nm).

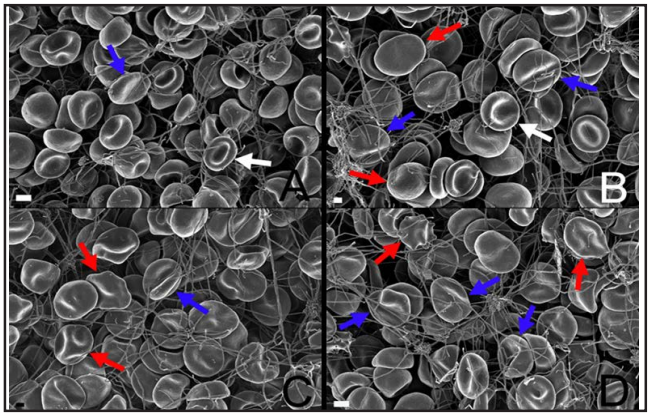

Fig. 4. Representative scanning electron micrographs of WB with thrombin of the control and metal exposed groups. Fig.s A (control), B (Cd), C (Cr) and D (Cd and Cr) indicate the erythrocyte and fibrin fibre interactions. White arrow: Normal erythrocytes; Red arrow: Variations in erythrocyte morphology; Blue arrows: Interactions between erythrocytes and fibrin fibres (Scale bars: B and C: 1µm; A and D: 2µm).

Table 2. Summary of SEM analysis on erythrocytes, platelets and fibrin networks; +, no or minimal change occurred; ++, some cell or fibre changes were visible; +++, most cells or fibres were altered; ++++, all cells or fibres were altered. WB+T: Whole blood with thrombin; PRP+T: Platelet rich plasma with thrombin

	Erythrocytes				Platelets		Fibrin network	
	WB		WB+T		PRP		PRP+T	
Groups	Altered erythrocyte morphology	Membrane disruption	Altered erythrocyte morphology	Changes due to interaction with fibrin fibres	Altered platelet morphology	Membrane disruption	Altered fibre morphology	Dense net-like appearance present
Control	++	+	++	+	++	+	+	+
Cd	+++	++	+++	++	++++	++	++	+
Cr	+++	+	+++	++	++++	++	++	+
Cd + Cr	+++	+	+++	++	++++	+++	++	++

Confocal laser scanning microscopy

In the negative control group, minimal positive Annexin V signal was obtained (Fig. 6 A-C). In the positive control, containing erythrocytes exposed to Mellitin (Fig. 6 D-F), an Annexin V positive signal was observed. Figures 7 A-F are examples of the type of Annexin V positive signal that was obtained in all the metal exposed groups. PS flip positive cells were scattered throughout the samples. The occurrence of the Annexin V PS flip positive cells

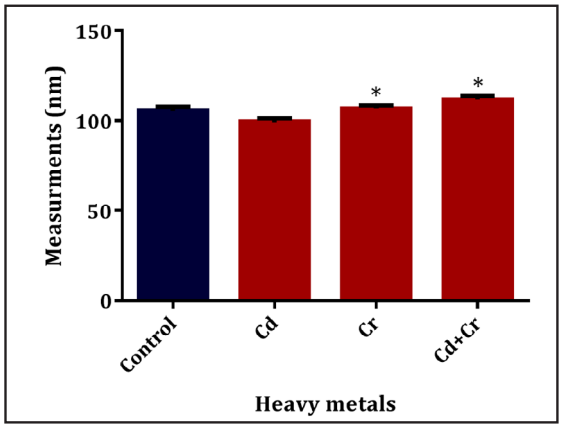

Fig. 5. Fibrin fibre diameter measurements. *Statistically significant compared to Cd; p-value of ≤0.05.

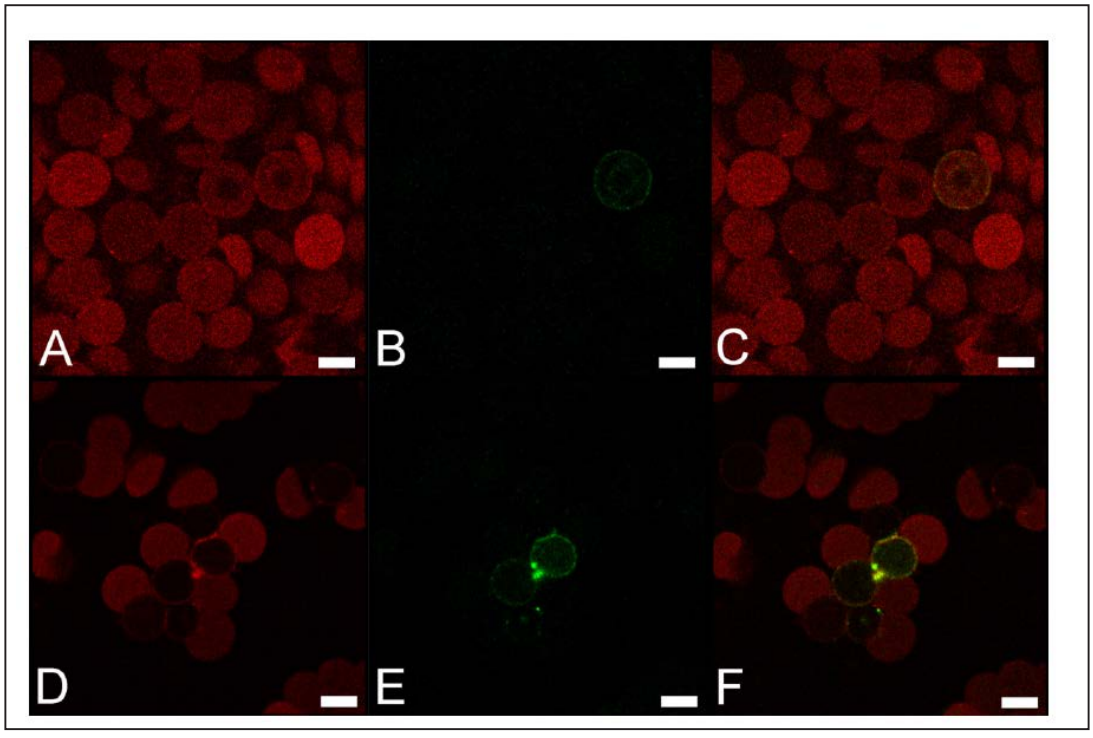

Fig. 6. Confocal laser scanning micrographs of the negative control (A-C) and positive control (D-F). Fig.s A and D showing the auto-fluorescence of the erythrocytes, B and D indicating the Annexin V signal obtained and C and F showing the overlay images (Scale bars: 5µm).

appears to be slightly increased in the metal combination groups, compared to the Cd and Cr groups. The Annexin V positive erythrocytes are mainly present in the spherocytes and not echinocytes (Fig. 7 A-F, green fluorescence).

Viscoelasticity

Fig. 8 shows representative traces of all the groups from which the r-time, k-time, α angle and MA was determined. Table 3 is a summary of the control and metal exposed group's viscoelastic profiles after exposure to Cd and Cr alone and in combination (mean ± standard deviation). No statistical significant difference in any of the parameters measured with TEG® could be found between the control group and metal exposed groups (Table 3) using the one-way ANOVA and Tukey's multiple comparisons test. Although no statistical significates

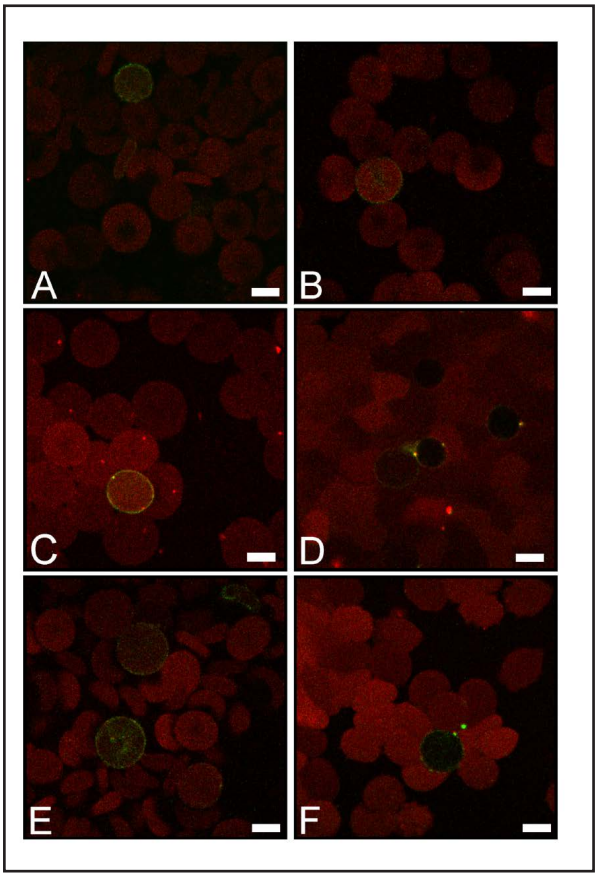

Fig. 7. PS exposure evaluation of erythrocytes after exposure to the heavy metals Cd and Cr alone and in combination using the confocal laser scanning microscope. Fig.s A - F indicate the Annexin V positive erythrocytes after exposure to Cd (A and B), Cr (C and D) and Cd and Cr (E and F) (Scale bars: 5µm).

were obtained, there was a visible trend in all the parameters of the metal groups.

The R and K values had a slight increase and the α angle and MA values decreased with the metal exposed groups. The velocity curve (v-curve) results, namely the MRTG, TMRTG and TTG, further confirms the trend seen with a decrease in the MRTG and TTG, correlating to the α angle and MA results and the TMRTG confirming the R value results.

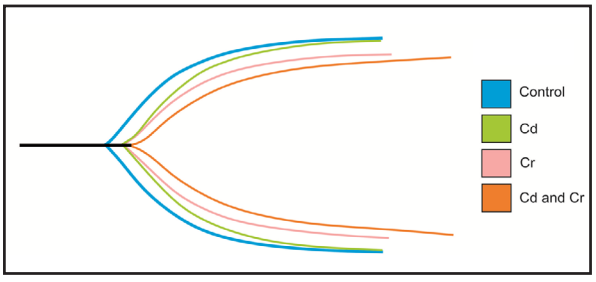

Fig. 8. Representative viscoelastic traces of the control and metal groups.

Discussion

Blood is an important component involved in the distribution of heavy metals like Cd and Cr to organs such as the liver and kidneys which are common sites of damage [24]. During this process of distribution these metals can adversely affect blood homeostasis, altering the structure and functioning of the cellular component of blood that includes the erythrocytes, platelets and the fibrin networks. In this study, an *ex vivo* model was used to evaluate the effects of Cd and Cr alone and in combination. Exposure concentrations of Cd was similar to that used by Sopjani et al. where exposure of a packed erythrocyte volume to 27.3µM for 48 hours caused 25% erythrocyte PS exposure and 5% haemolysis [34]. In the present study, WB was exposed to 26µM Cd for 10 minutes. Lupescu et al. exposed 0.4% haematocrit erythrocytes to 20µM Cr(VI) for 48hrs [35]. Erythrocyte haemolysis was 1% and PS exposure was 15%. WB haematocrit for healthy males is 42% [36] and therefore using WB, exposure to 200µM Cr(VI) would theoretically provide the same results. In the present study erythrocytes in WB were exposed to 5 fold higher Cr(VI) concentration's for only 10 minutes. PS exposure and associated changes in Ca^{2+} and erythrocyte morphology, after exposure to Cd and Cr alone and in combination, may adversely affect blood coagulation parameters. The focus of this a study is to determine the effect of blood coagulation providing an indication of possible thrombotic risk following exposure.

Cd and Cr alone and in combination caused ultrastructural changes (Fig. 1-4), to erythrocyte, platelet and fibrin fibre morphology (Fig. 1-4) compared to the controls. The increase in platelet activation, seen with the presence of pseudopodia and membrane

Table 3. Summary of the effects of Cd and Cr alone and in combination on the viscoelastic parameters; *statistical significance: p-value of ≤0.05. SD: Standard deviation

Parameter	Normal ranges	Control		Cd		Cr		Cd and Cr	
		Range	Mean ± SD	Range	Mean ± SD	Range	Mean ± SD	Range	Mean ± SD
R (min)	9-27	6.50-11.70	8.83 ± 1.89	7.10-12.30	9.62 ± 1.96	8.50-13.20	10.30 ± 1.77	6.40-13.10	9.98 ± 2.49
K (min)	2-9	2.60-4.50	3.73 ± 0.82	2.80-5.80	3.97 ± 1.10	3.50-4.90	4.35 ± 0.63	4.20-7.10	5.0 ± 1.10
α angle (deg)	22-58	27.40-57.00	42.42 ± 11.11	33.50-46.80	44.20 ± 8.61	34.70-46.80	40.10 ± 5.34	20.60-42.50	31.70 ± 8.46
MA (mm)	44-64	42.30-57.31	47.35 ± 5.46	41.70-51.10	45.72 ± 3.26	38.70-48.90	42.72 ± 3.61	37.10-47.50	42.52 ± 3.67
MRTG (Dynes/cm²/s)	0-10	2.56-12.06	4.53 ± 3.72	2.10-7.71	3.61 ± 1.80	2.42-3.54	2.78 ± 0.42	2.18-2.75	2.45 ± 0.20
TMRTG (min)	5-23	8.08-15.67	12.14 ± 2.58	10.00-18.50	12.71 ± 3.36	10.00 ± 16.33	12.93 ± 2.48	9.67-16.75	13.10 ± 2.84
TTG (Dynes/s²)	251-1014	366.56-674.67	460.49 ± 112.92	357.43-524.22	424.43 ± 58.02	317.12-481.22	377.76 ± 58.26	296.51-453.38	373.94 ± 55.84

spreading, were seen in the metal exposed groups that may cause a decrease in taut fibres and thus an increase in loose or bended fibres. Oxidative stress and inflammation is known to cause platelet activation that can cause pathological thrombi [14, 25, 37]. With the activation of platelets, agonists involved in the formation and stability of clot are released and include adenosine diphosphate (ADP), serotonin, thrombin and thromboxane A_2 [14, 37]. Platelets also play a crucial role in fibrin formation and tautness, thus the bent fibres seen in the fibrin networks of the metal groups might be due to the platelet functional changes or lack of thrombin production [25]. The significant increase in fibre thickness in the metal groups will further contribute to the alterations of the erythrocytes and clot formation, as it might cause a reduction in the lysis of the clots [38]. The alteration in fiber thickness can be due to the transition of the fibers α-helices into β-sheets and protein aggregation [33]. Fibrin fibres consist of an combination of α-helices, β-sheets and turns, loops and random coils which contributes to the normal structure and function of the fibrin fibres [33].

Cd and Cr alone and in combination caused changes in erythrocyte morphology and this was associated with increased expression of Annexin V. Cd and Cr cause oxidative stress in the cells via different biochemical pathways. Cd binds sulfhydryl groups of proteins and glutathione (GSH) and especially GSH depletion results in increased production of reactive oxygen species (ROS) such as hydrogen peroxide, superoxide anion and hydroxyl radical [39-42]. Cr in contrast enters the redox cycle and acts as a catalyst of the Fenton reaction involving H_2O_2, leading to an increase in ROS production and alters erythrocyte membrane fluidity and integrity making erythrocytes more fragile and less osmotic resistant [40, 43]. Gao et al. observed following exposure of erythrocytes to increasing concentration of betulinic acid, erythrocyte morphology changed from normal, to a mixture of normal, early discocyte-echinocytes (biconcave disk to star-shape), discocyte-stomatocytes (biconcave disk to cup-shape), echinocytes, echinocytes with vesicles, spherocytes and a few stomatocytes [44]. Likewise, a mixture of erythrocyte morphologies was observed in the present study. Low Annexin-V binding was associated with echinocytes (erythrocytes with regularly spaced short projections or spicules) and knizocytes (elevated or elongated pinched area in the centre of the erythrocytes), with regular peripheral Annexin V signal associated with the spherocytes (swollen, spherical erythrocytes). Ultrastructural results, together with the results from CLSM, that indicated that the Annexin V positive signals were mainly found on the spherocytic erythrocytes exposed to Cd and Cr in combination. Lupescu et al. reported that erythrocytes exposed to 54.5μM for 48 hours observed that only 40% erythrocytes bound Annexin

V. Likewise, Sopjani et al. 20µM Cr(VI) for 48 hours resulted in positive in 12% erythrocytes staining positive for Annexin V [34, 35].

The Annexin V signals seen in this study might be due to the increase in influx of Ca^{2+} into the erythrocytes, activation of the Ca^{2+}/K^{+} channels and ATP depletion that are initiated by oxidative stress caused by the Cr and to lessor degree Cd [11, 34, 35, 45]. The increase in cytosolic Ca^{2+} will activate scramblase in the erythrocytes, which inhibits flippase that in turn causes floppase to translocate PS to the outside, resulting in the PS flip and membrane scrambling (Fig. 9). Besides the Ca^{2+} that activates scramblase, it also affects the sensitive Ca^{2+}/K^{+} channels which causes KCl exiting the cells together with water and thus causing cell shrinkage (Fig. 9) [34, 35, 45]. Ca^{2+} entering the cells can also lead to the activation of Calpain, a cysteine endopeptidase that degrades membrane proteins, leading to membrane blebbing (Fig. 9) [11]. Energy depletion also initiated by an increase in cytosolic Ca^{2+} and can also contribute to eryptosis. Although both Cd and Cr both have different mechanisms of toxicity, the consequence thereof is similar resulting in eryptosis, which is increased due to a concentration effect when erythrocytes are exposed to Cd and Cr in combination.

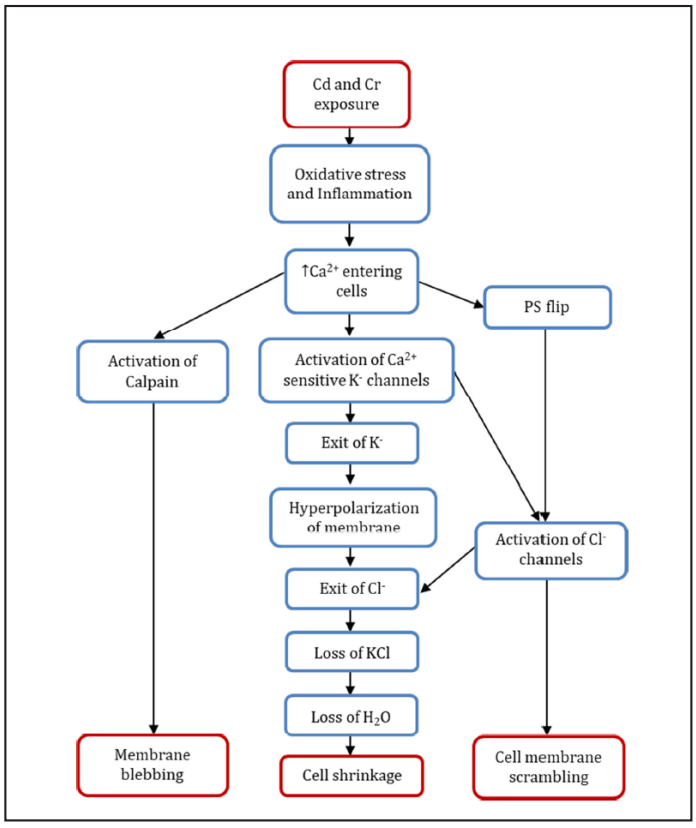

Fig. 9. Summary of erythrocyte pathology (Modified from: [46]).

TEG® is widely used in trauma care to evaluate whole blood coagulation [47]. In a recent study by Lehnert et al. [48], analysis of acute pulmonary embolisms, the mean values of TEG® were within normal ranges. Likewise in the present study acute exposure to Cd and Cr alone and in combination provides TEG® results within the normal range (Table 3). However evaluation of the viscoelastic traces Cd and Cr alone and in combination (Fig. 8) indicates that these heavy metals cause minor although no statistically significant changes to the measured parameters. The trend seen in the viscoelastic results indicate that the R value slightly increased, thus resulting in a delayed fibrin formation. Fibrin formation is catalysed by the enzyme thrombin from fibrinogen and stabilized by thrombin-catalysed factor XIII (FXIII) [33]. Both these components depend on the presence of calcium, as calcium is a co-factor in the formation of FXIII and thrombin and it is known that heavy metals deplete calcium levels [15, 49]. The increased trend seen in K time indicates that the initial clot formation, after it starts forming is rapid. This correlates with the activated platelets seen with SEM analysis (Fig. 2). The decrease in both the α angle and MA values indicates that the fibrin build up is slower due to the reduction in fibrin cross-linking, which results in a fragile, less-stable clot. The clot strength is also decreased as the platelet-fibrinogen interactions are decreased (Table 3) which also correlates with the SEM results, as the fibres appear to be less taut (Fig. 3). This is further supported by the v-curve data. The TMRTG shows that the total clot formation, from start to maximum clot formation takes longer and correlates with

the longer time for initial clot formation as observed with increased R value. The decrease in MRTG and TTG also indicates that clot formation will be slower and weaker. This fragile clot may cause problems in the cardiovascular system, as these weak clots may detach and cause a blockage in an artery or vein leading to thrombosis.

Cigarette smoking has been shown to increase fibrin fibre thickness and platelet activation and cause erythrocyte alterations [50-52]. Cigarette smoke is a complex mixture of more than 4000 components that has been identified in mainstream cigarette smoke, this includes heavy metals such as Cd and Cr and the present study clearly shows that Cd and Cr contributes to this effect [53, 54]. Likewise exposure to these metals in water and polluted air can also contribute to increased risk for thrombosis. Although this *ex vivo* study investigated the effect of a 1000 times of a single acute dosage, this study clearly identifies the blood as a target of toxicity prior to metabolism in the liver and excretion by the kidneys. Furthermore, accumulative effects of low levels of each metal as part of complex mixtures may also adversely affect blood coagulation. Evaluation of the morphology of blood components may be an important technique that can be used to identify early morphological changes prior to the identification of altered coagulation using standard clinical methods.

Conclusion

Cd and Cr alone and in combination causes increased platelet activation, abnormal fibrin network formation and Annexin V positive signal. The TEG® analysis, although not statistically significant, indicated that the final clot will probably result in a fragile and less stable clot. This study identifies the blood as an important target system of Cd and Cr toxicity.

Acknowledgements

The authors would like to thank the National Research Foundation (NRF) for their financial support (Grant number: 92768). Staff of the Department of Physiology of the University of Pretoria that assisted with phlebotomy and TEG® analysis and all the volunteers that generously donated blood required for this study.

Disclosure Statement

The authors declare no conflict of interest.

References

1 Smith SA: The cell-based model of coagulation. J Vet Emerg Crit Car 2009;19:3-10.
2 Zhang W, Houb ST, Stanimirovic D: Blood Brain Barrier Protection in Stroke: Taming tPA; The Blood-Brain Barrier in Health and Disease, Volume Two: Pathophysiology and Pathology, 2015, pp 226-246.
3 Van Rooy M-J: Blood coagulation in metabolic syndrome-induced transient ischemic attack: Department of Physiology. Pretoria, South Africa, University of Pretoria, 2015, PhD,
4 Pérez-Gómez F, Bover R: The new coagulation cascade and its possible influence on the delicate balance between thrombosis and hemorrhage. Rev Esp Cardiol 2007;60:1217-1219.
5 Föller M, Huber SM, Lang F: Erythrocyte programmed cell death. IUBMB life 2008;60:661-668.
6 Lang F, Gulbins E, Lang PA, Zappulla D, Föller M: Ceramide in suicidal death of erythrocytes. Cell Physiol Biochem 2010;26:21-28.
7 Lang F, Lang E, Föller M: Physiology and pathophysiology of eryptosis. Transfusion Medicine and Hemotherapy 2012;39:308-314.

8 Lang F, Qadri SM: Mechanisms and significance of eryptosis, the suicidal death of erythrocytes. Blood Purif 2012;33:125-130.
9 Mischitelli M, Jemaa M, Almasry M, Faggio C, Lang F: Ca2+ Entry, Oxidative Stress, Ceramide and Suicidal Erythrocyte Death Following Diosgenin Treatment. Cell Physiol Biochem 2016;39:1626-1637.
10 Pretorius E, du Plooy JN, Bester J: A Comprehensive Review on Eryptosis. Cell Physiol Biochem 2016;39:1977-2000.
11 Pretorius E, Swanepoel AC, Buys AV, Vermeulen N, Duim W, Kell DB: Eryptosis as a marker of Parkinson's disease. Aging 2014;6:788-819.
12 Pretorius E, Kell DB: Diagnostic morphology: biophysical indicators for iron-driven inflammatory diseases. Integrative Biology 2014;6:486-510.
13 Gorbet MB, Sefton MV: Biomaterial-associated thrombosis: roles of coagulation factors, complement, platelets and leukocytes. Biomaterials 2004;25:5681-5703.
14 van Rooy M-J, Pretorius E: Metabolic syndrome, platelet activation and the development of transient ischemic attack or thromboembolic stroke. Thromb Res 2015;135:434-442.
15 Swanepoel AC, Nielsen VG, Pretorius E: Viscoelasticity and ultrastructure in coagulation and inflammation: two diverse techniques, one conclusion. Inflammation 2015;38:1707-1726.
16 Lang E, Qadri SM, Lang F: Killing me softly–suicidal erythrocyte death. Int J Biochem Cell Biol 2012;44:1236-1243.
17 Pretorius E, Bester J, Vermeulen N, Alummoottil S, Soma P, Buys AV, Kell DB: Poorly controlled type 2 diabetes is accompanied by significant morphological and ultrastructural changes in both erythrocytes and in thrombin-generated fibrin: implications for diagnostics. Cardiovasc Diabetol 2015;14:1.
18 Ambrose JA, Barua RS: The pathophysiology of cigarette smoking and cardiovascular disease: an update. J Am Coll Cardiol 2004;43:1731-1737.
19 Hoek G, Brunekreef B, Fischer P, van Wijnen J: The association between air pollution and heart failure, arrhythmia, embolism, thrombosis, and other cardiovascular causes of death in a time series study. Epidemiology 2001;12:355-357.
20 Swanepoel AC, Visagie A, de Lange Z, Emmerson O, Nielsen VG, Pretorius E: The clinical relevance of altered fibrinogen packaging in the presence of 17β-estradiol and progesterone. Thromb Res 2016;146:23-34.
21 Prozialeck WC, Edwards JR: Mechanisms of cadmium-induced proximal tubule injury: new insights with implications for biomonitoring and therapeutic interventions. J Pharmacol Exp Ther 2012;343:2-12.
22 Langárd S, Costa MAX: Chromium; in Nordberg GF, Fowler BA, Nordberg M (eds): Handbook on the Toxicology of Metals Burlington, Academic Press, 2007, pp 487-510.
23 Zhou Z, Lu Y-h, Pi H-f, Gao P, Li M, Zhang L, Pei L-p, Mei X, Liu L, Zhao Q: Cadmium Exposure is Associated with the Prevalence of Dyslipidemia. Cell Physiol Biochem 2016;40:633-643.
24 Venter C, Oberholzer HM: An *in ovo* investigation of the cellular effects of the heavy metals cadmium and chromium alone and in combination: Anatomy. Pretoria, South Africa, University of Pretoria, 2015, Masters,
25 van Rooy M-J, Duim W, Ehlers R, Buys AV, Pretorius E: Platelet hyperactivity and fibrin clot structure in transient ischemic attack individuals in the presence of metabolic syndrome: a microscopy and thromboelastography® study. Cardiovasc Diabetol 2015;14:86.
26 W.H.O: Guidelines for drinking-water quality World Health Organization: World Health Organization. Switzerland, 2011, 2015,
27 Han SM, Lee KG, Yeo JH, Hwang SJ, Jang CH, Chenoweth PJ, Pak SC: Effects of bee venom treatment on growth performance of young pigs. The American journal of Chinese medicine 2009;37:253-260.
28 Park C, Lee DG: Melittin induces apoptotic features in Candida albicans. Biochem Biophys Res Commun 2010;394:170-172.
29 Park JH, Jeong Y-J, Park K-K, Cho H-J, Chung I-K, Min K-S, Kim M, Lee K-G, Yeo J-H, Park K-K: Melittin suppresses PMA-induced tumor cell invasion by inhibiting NF-κB and AP-1-dependent MMP-9 expression. Mol Cells 2010;29:209-215.
30 Larsen CC, Hansen-Schwartz J, Nielsen JD, Astrup J: Blood coagulation and fibrinolysis after experimental subarachnoid hemorrhage. Acta Neurochir (Wien) 2010;152:1577-1581.
31 Shin K-H, Kim I-S: Thromboelastographic Evaluation of Coagulation in Patients with Liver Disease. Blood 2015;126:1089-1089.

32 Wiinberg B, Jensen AL, Rojkjaer R, Johansson P, Kjelgaard Hansen M, Kristensen AT: Validation of human recombinant tissue factor–activated thromboelastography on citrated whole blood from clinically healthy dogs. Vet Clin Pathol 2005;34:389-393.
33 Kell DB, Pretorius E: Proteins behaving badly. Substoichiometric molecular control and amplification of the initiation and nature of amyloid fibril formation: lessons from and for blood clotting. Prog Biophys Mol Biol 2016:1-26.
34 Sopjani M, Föller M, Dreischer P, Lang F: Stimulation of eryptosis by cadmium ions. Cell Physiol Biochem 2008;22:245-252.
35 Lupescu A, Jilani K, Zelenak C, Zbidah M, Qadri SM, Lang F: Hexavalent chromium-induced erythrocyte membrane phospholipid asymmetry. Biometals 2012;25:309-318.
36 Brun J, Bouchahda C, Chaze D, Aïssa Benhaddad A, Micallef J, Mercier J: The paradox of hematocrit in exercise physiology: which is the "normal" range from an hemorheologist's viewpoint? Clin Hemorheol Microcirc 2000;22:287-303.
37 Freedman JE: Oxidative stress and platelets. Arterioscler Thromb Vasc Biol 2008;28:s11-s16.
38 Swanepoel AC, Visagie A, Pretorius E: Synthetic Hormones and Clot Formation. Microsc Microanal 2016;22:878-886.
39 Bertin G, Averbeck D: Cadmium: cellular effects, modifications of biomolecules, modulation of DNA repair and genotoxic consequences (a review). Biochimie 2006;88:1549-1559.
40 Stohs S, Bagchi D: Oxidative mechanisms in the toxicity of metal ions. Free Radic Biol Med 1995;18:321-336.
41 Hu K-H, Li W-X, Sun M-Y, Zhang S-B, Fan C-X, Wu Q, Zhu W, Xu X: Cadmium induced apoptosis in MG63 cells by increasing ROS, activation of p38 MAPK and inhibition of ERK 1/2 pathways. Cell Physiol Biochem 2015;36:642-654.
42 Chen Z-Y, Liu C, Lu Y-h, Yang L-L, Li M, He M-D, Chen C-H, Zhang L, Yu Z-P, Zhou Z: Cadmium exposure enhances bisphenol A-induced genotoxicity through 8-oxoguanine-DNA glycosylase-1 OGG1 inhibition in NIH3T3 fibroblast cells. Cell Physiol Biochem 2016;39:961-974.
43 Husain N, Mahmood R: Hexavalent chromium induces reactive oxygen species and impairs the antioxidant power of human erythrocytes and lymphocytes: Decreased metal reducing and free radical quenching ability of the cells. Toxicol Ind Health 2017:0748233717703892.
44 Gao M, Lau P, Kong S: Mitochondrial toxin betulinic acid induces *in vitro* eryptosis in human red blood cells through membrane permeabilization. Arch Toxicol 2014;88:755-768.
45 Pretorius E, Oore-ofe O, Mbotwe S, Bester J: Erythrocytes and their role as health indicator: Using structure in a patient-orientated precision medicine approach. Blood Rev 2016
46 Pretorius E, Oore-ofe O, Mbotwe S, Bester J: Erythrocytes and their role as health indicator: Using structure in a patient-orientated precision medicine approach. Blood Rev 2016;30:263-274.
47 Bolliger D, Seeberger MD, Tanaka KA: Principles and practice of thromboelastography in clinical coagulation management and transfusion practice. Transfus Med Rev 2012;26:1-13.
48 Lehnert P, Johansson PI, Ostrowski SR, Møller CH, Bang LE, Olsen PS, Carlsen J: Coagulopathy in patients with acute pulmonary embolism: a pilot study of whole blood coagulation and markers of endothelial damage. Scand J Clin Lab Invest 2017;77:19-26.
49 Timbrell J: Principles of Biochemical Toxicology, ed 3. CRC Press, 1999.
50 Pretorius E, Oberholzer HM, van der Spuy WJ, Meiring JH: Smoking and coagulation: the sticky fibrin phenomenon. Ultrastruct Pathol 2010;34:236-239.
51 Armani C, Landini Jr L, Leone A: Molecular and biochemical changes of the cardiovascular system due to smoking exposure. Curr Pharm Des 2009;15:1038-1053.
52 Pretorius E, du Plooy JN, Soma P, Keyser I, Buys AV: Smoking and fluidity of erythrocyte membranes: A high resolution scanning electron and atomic force microscopy investigation. Nitric Oxide 2013;35:42-46.
53 Fresquez MR, Pappas RS, Watson CH: Establishment of toxic metal reference range in tobacco from US cigarettes. J Anal Toxicol 2013;37:298-304.
54 Dallüge J, Van Stee LL, Xu X, Williams J, Beens J, Vreuls RJ, Udo A: Unravelling the composition of very complex samples by comprehensive gas chromatography coupled to time-of-flight mass spectrometry: Cigarette smoke. J Chromatogr A 2002;974:169-184.